Phenomenal Insight into Electrochemically Induced Photocatalytic Degradation of Nitrobenzene on Variant Au-Modified TiO$_2$ Nanotubes

Meng Wang [1], Chaoying Li [1,2], Yingdong Wang [2], Di Gu [2,*] and Baohui Wang [1,*]

[1] Institute of New Energy Chemistry and Environmental Science, College of Chemistry and Chemical Engineering, Northeast Petroleum University, Daqing 163318, China

[2] National Key Laboratory of Continental Shale Oil, Northeast Petroleum University, Daqing 163318, China

* Correspondence: gudi@nepu.edu.cn (D.G.); wangbh@nepu.edu.cn (B.W.)

Abstract: TiO$_2$ nanotubes are a prominent type of TiO$_2$-based nanostructure compared to nanorod arrays. A promising way to improve photocatalytic performance is modifying TiO$_2$ nanotubes with metals, either on the surface or inside the tubes. There is a substantial demand for enhancing the conductivity and charge separation of TiO$_2$ nanotubes, with a major focus on gold (Au) modification. Gold (Au) coatings have significantly improved the photocatalytic activity of TiO$_2$ nanotubes, particularly in pollutant oxidation. However, the mechanism underlying the action of Au-modified TiO$_2$ nanotubes in photocatalytic nitrobenzene oxidation under electrochemical induction remains unclear. Therefore, we conducted related experiments to explore the optimal Au concentration under various conditions. Under electric field induction, the maximum removal rate achieved was 54.9%. Lastly, we analyzed the relevant photocatalytic mechanism to elucidate the responses of electrons and holes to a simulated contaminant under a photo-electrochemical field.

Keywords: photocatalysis; Au-modified TiO$_2$ nanotubes; organic wastewater degradation; photocatalytic mechanism; photo-electrochemical field

1. Introduction

TiO$_2$, a well-known catalyst, offers several advantages, such as non-toxicity, exceptional chemical durability, and favorable photocatalytic activity, especially in the degradation of organic contaminants in industrial effluents. It has been extensively employed in environmental protection. However, its wide bandgap of 3.2 eV and rapid carrier recombination behavior significantly limit its practical application in the field of solar energy. To effectively reduce the bandgap and enhance visible light adsorption, various strategies have been employed during the synthesis process, including defect introduction, specific element doping, and semiconductor incorporation. For instance, incorporating g-C$_3$N$_4$ into TiO$_2$ can lead to the formation of a heterojunction structure, including the traditional Type II [1] and Z scheme [2], effectively altering the movement of charge carriers. Introducing defects to reduce the bandgap can enhance visible light absorption [3]. In general, the most commonly employed approaches to augmenting photocatalytic activity entail the application of noble metals or metal doping. This is primarily due to their facile integration into the titanium dioxide lattice via photo-reduction or electrochemical deposition. These doping techniques are frequently characterized by their simplicity and high efficiency. Additionally, the utilization of nanoscale particles has proven to be highly effective in enhancing photocatalytic activity, despite the fact that the precise mechanism underlying this nanoscale effect remains to be fully comprehended. For instance, noble metals such as Pt, Ag, or Au have been dispersed into nano-sized particles to optimize titanium dioxide, addressing the previously mentioned drawbacks [4–6]. Due to their strong light absorption capabilities, Au nanoparticles induce electrons to transition from the 5d level to the 6s

level, leading to a significant characteristic absorption band in the visible light spectrum, centered around 560 nm. Based on the plasma resonance (SPR) effect [7] between the excited electrons and the Au from the surface of the nanotubes, Au nanoparticles capture photo-induced electrons excited by light, restraining the complex of the electrons and holes, increasing the photocatalytic activity of the composites.

Numerous studies have explored the modification of TiO_2 with Au using various methods. Tran [8] utilized pulsed laser ablation to reduce Au^+ to Au and carried out a series of processes to deposit Au nanoparticles onto a TiO_2 substrate. Furthermore, the preparation method, which was both time consuming and complex, significantly reduced the catalytic effects during the degradation reaction. A suspension was prepared by immersing powdered TiO_2 in a solution containing Au [9] and coating it onto sol–gel produced vitreous quartz microscope slides. Despite the material having a higher specific surface area and better adherence, its practical application was still hindered by lower repeatability and recoverability to some extent. The synthesis of TiO_2 nanotubes through the hydrothermal method involved immersing them in solutions with varying concentrations of $HAuCl_4 \cdot 4H_2O$, followed by preparing the mixture through calcination [9]. Although this method improved the degradation efficiency of the catalyst, it consumed a significant amount of time and resulted in uneven scattering of Au. Li [10] deposited Au particles on fluorine-doped tin oxide (FTO) containing TiO_2 nanorods using an electrochemical method, expanding the visible region and improving utilization efficiency. Doping Co on TiO_2 nanotubes as the anode [11] resulted in the degradation of MB into inorganic substances when an electrochemical method was used. This approach significantly enhanced degradation efficiency and reduced carrier recombination. However, in many studies concerning the surface modification of Au [12,13] on TiO_2, there has been limited research on the optimal loading amount and the degradation of organic substances under a photo-electro field [14–16].

The advancement of electrochemical techniques has led to the emergence of the electro-photo coupling field as a promising tool for enhancing the efficiency of degradation processes. Photoelectrochemical (PEC) processes, known for their simplicity, high efficiency, and low pollution, have gained increasing attention from scientific researchers. These processes primarily focus on minimizing electron–hole recombination, maximizing utilization efficiency, and amplifying catalytic activity. Lsy and his colleagues [17] fabricated Ti/black TiO_2/PbO_2 micro/nanostructure photoelectrodes that exhibited good degradation efficiency for anthraquinone dye under an external electric field and a supplied light source. Yang et al. [18] used hydrothermal methods to synthesize MoS_2/TiO_2 materials for the treatment of chromium-containing wastewater. At a concentration of 300 mg/L, the degradation efficiency for the model pollutant reached 90% through the electro-photo effect. Gao et al. [19] constructed CdS-TiO_2 nanocomposite-based sensors capable of combining a photoelectrochemical to detect nitrite. These materials, with a photo-electro function, exhibited characteristics of good stability, reusability, and excellent sensing capabilities. Gong et al. [20] synthesized highly ordered Cr-doped titania nanotube arrays that displayed good performance for the degradation of methyl orange under Xe lamp illumination. Lin and her research group [21] utilized highly dispersed TiO_2 with graphene oxide sheets for the oxidation of ethanol, integrating photo-electro processes to reduce recombination between TiO_2 and graphene oxide and enhance favorable properties. Compared to physical or chemical processes, photo-electron catalysis can be considered an effective approach [22].

To explore the photocatalytic and photoelectrocatalytic properties of Au/TiO_2 nanotubes, nitrobenzene, a common component in organic wastewater, was selected to evaluate the catalytic efficacy of Au/TiO_2 nanotubes with varying Au loadings.

Both the photocatalytic (PC) and photoelectrocatalytic (PEC) performance of the Au/TiO_2 nanotubes were investigated with respect to the removal efficiency of nitrobenzene in the wastewater systems. By varying the Au loading, Au/TiO_2 nanotubes exhibited improved catalytic activity under photoelectrocatalytic conditions. The results indicated a significant improvement in catalytic activity and catalyst lifespan for Au-modified Ti-based

Au/TiO$_2$ nanotubes in both PC and PEC conditions. Taking into account relevant references and previous studies, a probable mechanism based on the active substances in the reaction is presented, providing further insights into the nature of PC and PEC.

2. Results and Discussion

Figure 1a shows an SEM image of pristine TiO$_2$ nanotubes, revealing the inner TiO$_2$ nanotubes' highly ordered array structures. An inerratic hexagonal structure with a diameter of 150–2000 nm was observed on top of the material. Figure 1b–h are Au/TiO$_2$ nanotubes of different loading concentrations. Compared with the pristine TiO$_2$ nanotubes in Figure 1a, the top of the tube became thick when increasing the loading concentration of Au, allowing the active surface of the catalyst to significantly enhance the catalytic activity [23]. In Figure 1f, the morphology of the nanotubes and the loadings of Au nano-particles inside the tubes can be clearly observed, proving that the electrochemical deposition method was successfully used to load nanometallic particles onto the inner walls of the tubes, which can improve the photocatalytic effect. When the concentration reached 0.7 g/L (Figure 1g), a large number of Au particles block the pores on the top layer and induced the shielding of the active area of the TiO$_2$ nanotubes [24]. From this, it can be inferred that an appropriate gold loading can positively promote the photocatalytic effect of TiO$_2$ nanotubes. However, when the loading amount continues to increase, excessive gold on the surface can block the excitation of photons on the surfaces of TiO$_2$ nanotubes, thereby failing to promote the photocatalytic effect and possibly even weakening the original photocatalytic effect.
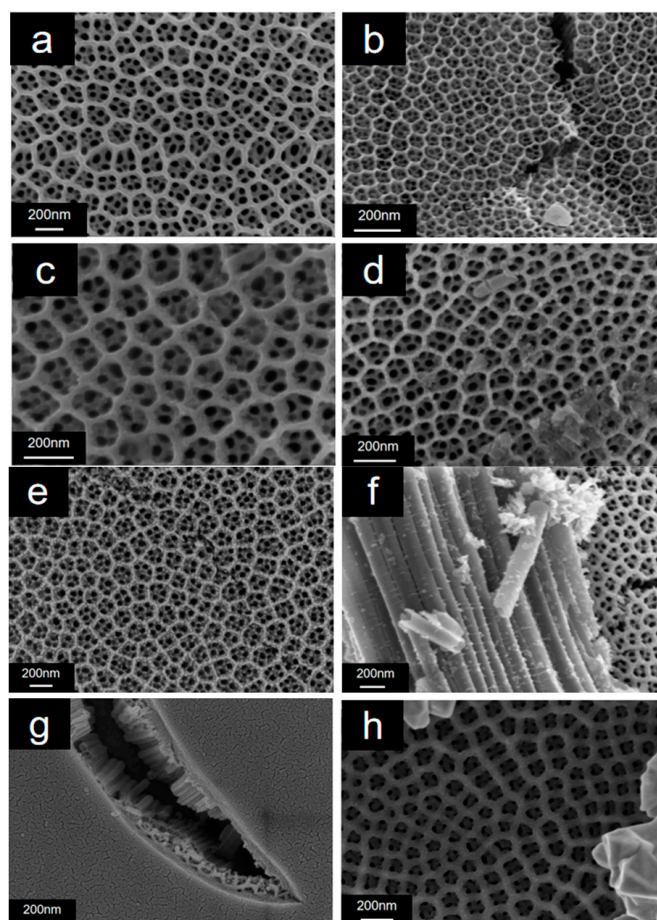

Figure 1. SEM: (**a**) TiO$_2$ nanotubes produced via two-step oxidation; (**b–h**) Au/TiO$_2$ nanotubes in doping amounts of 0.2, 0.3, 0.4, 0.5, 0.6, 0.7, and 0.8 g/L Au.

The elemental content was detected by EDS. As shown in Figure 2, the TiO_2 nanotubes consisted of Ti, O, and C. The appearance of the C peak was attributed to the reduction of CO_2 from the air [25] during the calcination process. Moreover, part of the EG was reduced by carrying out anodization. In the sample of the Au/TiO_2 nanotubes, successful loading of gold was (illustrated in Figure 2) noted by the characteristic peak of Au. In contrast with the different samples, the peak intensity of Au enhanced with a changing concentration.Since EDS can only be used to qualitatively and quantitatively analyze the microelements on a sample's surface, ICP-AES was employed to determine the overall elemental composition of the samples. Table 1 displays the mass fractions of each element, revealing that both Au/TiO_2 NTs are composed of Ti, Au, and O, and this composition aligns with our expectations. The mass fraction of Ti was slightly higher than that of Au. This can be attributed to the nanotubes on the titanium substrate and the deposited Au being primarily concentrated on the nanotubes, causing the titanium substrate to completely dissolve in the solution during ICP-AES measurement. The presence of Au in the Au/TiO_2 NTs confirms the successful introduction of Au into TiO_2 NTs. To further confirm the successful preparation of the material, other characterization methods were also applied.
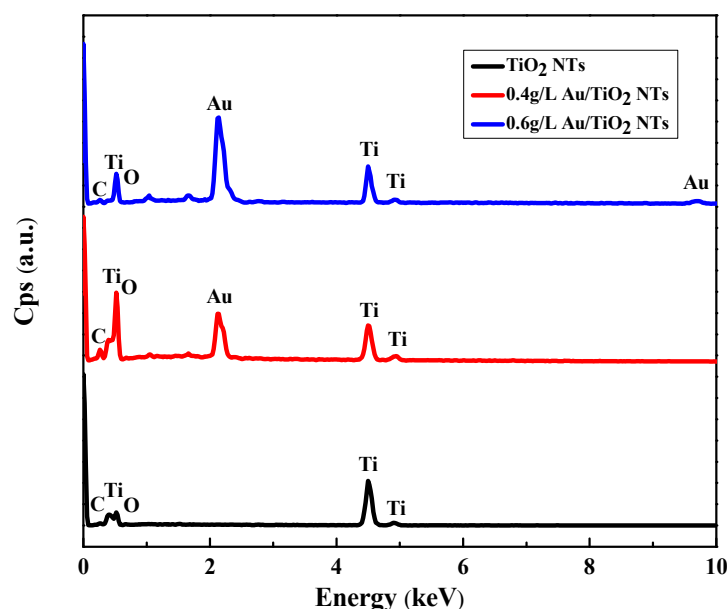

Figure 2. EDS spectra of TiO_2 nanotubes and Au/TiO_2 nanotubes with different doping concentrations.

Table 1. Mass fractions (%) of Au/TiO_2 NT samples.

Samples	Ti	O	Au
0.4 g/L Au/TiO_2 NTs	99.72	0.2832	0.0071
0.6 g/L Au/TiO_2 NTs	99.56	0.3424	0.0137

Figure 3 displays a series of XRD spectra obtained for the Au-doped and pristine TiO_2 nanotubes. It is known that TiO_2 has different crystalline phases, including anatase, rutile, and brookite. Among these phases, anatase exhibits the most excellent photocatalytic activity. The XRD pattern displayed common peaks, namely, (101), (004), (200), and (105), characteristic of anatase. Additional diffraction peaks, namely, (100), (110), and (103), corresponded to the Ti metal phase [26], indicating that the TiO_2 nanotubes consisted of a mixture of the anatase phase and Ti phase.
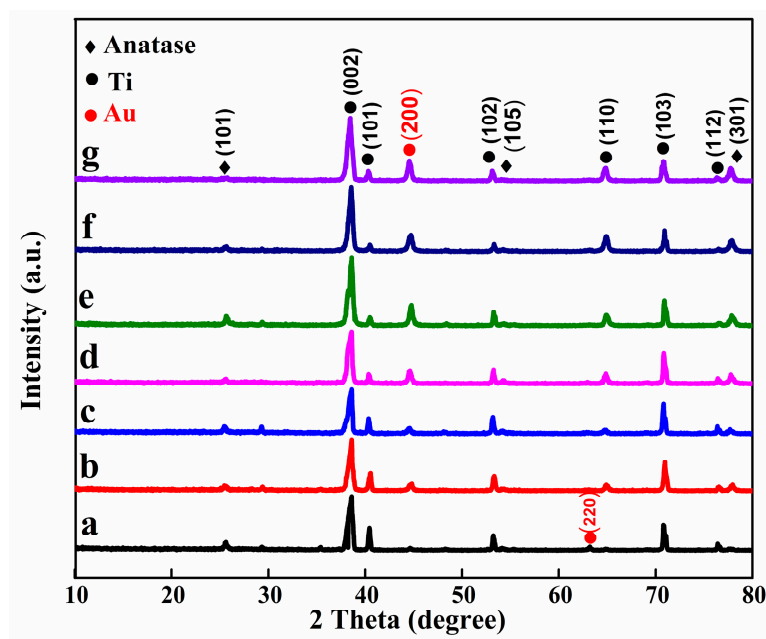
Figure 3. XRD patterns of (a) TiO_2 NTs; (b) 0.2 g/L Au@TiO_2 NTs; (c) 0.3 g/L Au@TiO_2 NTs; (d) 0.4 g/L Au@TiO_2 NTs; (e) 0.5 g/L Au@TiO_2 NTs; (f) 0.6 g/L Au@TiO_2 NTs; (g) 0.7 g/L Au@TiO_2 NTs.

In the case of the Au/TiO_2 nanotubes, they corresponded to the mixture phase and exhibited no significant differences from pristine TiO_2 nanotubes. The peaks at 2 theta values of 38.21°, 44.32°, and 63.80° match the (111), (200), and (220) planes [27] of the Au phase in the patterns (JCPDS 65-2870), confirming the presence of metallic Au. Further analyses, in combination with SEM and EDS, can demonstrate the successful preparation of Au/TiO_2 nanotubes.

To investigate the impact of ultraviolet (UV) light and gold concentrations on nitrobenzene degradation, cyclic voltammetry curves of the nitrobenzene solution were examined before and after UV light exposure. A conventional three-electrode system was employed in the experiment, with Au/TiO_2 nanotubes serving as the photoanode, Pt serving as the photocathode, and Ag/AgCl acting as the reference electrode. To emphasize the nitrobenzene characteristic peak, a high electrolyte concentration (1 g/L nitrobenzene) and 15 g/L of Na_2SO_4 serving as the supporting electrolyte were employed. In the experiment, a UV lamp was used as a light source, and the scanning rate was 50 mV/s during the whole experiment. The volt–ampere characteristic curve of the nitrobenzene solution was analyzed under the condition of avoiding light, and the detection results are shown in Figure 4a. The cyclic voltammetry curve of the nitrobenzene solution was analyzed under ultraviolet light, and the detection results are shown in Figure 4b. As can be seen from the two figures, the cyclic voltammetry curve of nitrobenzene is regular under the two conditions; only one obvious oxidation peak was detected in the positive direction of the scanning of nitrobenzene on each oxidation curve, and likewise, only one reduction peak was detected in a negative direction. This means that in this mode, nitrobenzene was oxidized in only one step. Upon comparing the two figures, it is evident that the oxidation and reduction peaks obtained with the Au/TiO_2 nanotubes loaded with Au were significantly higher than those of the two-step TiO_2 nanotubes. In comparison to the TiO_2 nanotubes, the chemical reaction was more pronounced under Au/TiO_2 nanotube conditions, making nitrobenzene more susceptible to oxidation. A comparison of the two figures reveals that the area under the cyclic voltammetry curve of nitrobenzene exposed to UV light was significantly larger than that under dark conditions, indicating a more intense chemical reaction under UV light, facilitating nitrobenzene oxidation.
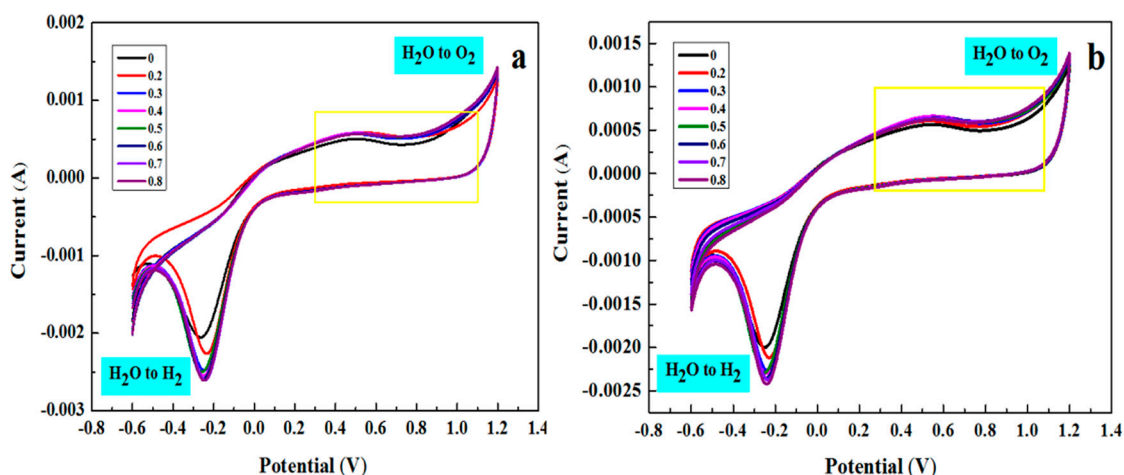
Figure 4. Cyclic voltammetry curves of nitrobenzene in the dark (**a**) and (**b**) under UV light.

UV-Vis spectroscopy was utilized to analyze the absorption properties of TiO_2 and Au/TiO_2 nanotubes. Figure 5 shows that the absorption intensity of the TiO_2 nanotubes and Au/TiO_2 nanotubes in the visible light region was lower than that in the UV light region. In comparison to the TiO_2 nanotubes, the Au/TiO_2 nanotubes exhibited superior absorption in the UV light region. Additionally, Au/TiO_2 nanotubes displayed notable absorption at 520 nm, which can be attributed to the surface plasmon resonance (SPR) effect of the Au nanoparticles. TiO_2 exhibited a negative conduction band at -0.5 V, while the Fermi level of the Au nanoparticles was 0.45 V. Therefore, when Au was incorporated into the TiO_2 nanotubes, the Au and TiO_2 nanotubes counteracted the negative and positive potentials, respectively, ultimately achieving an equilibrium [28]. Due to the SPR effect, electrons from Au nanoparticles can transfer to the conduction band of TiO_2, thereby enhancing catalytic performance [29].
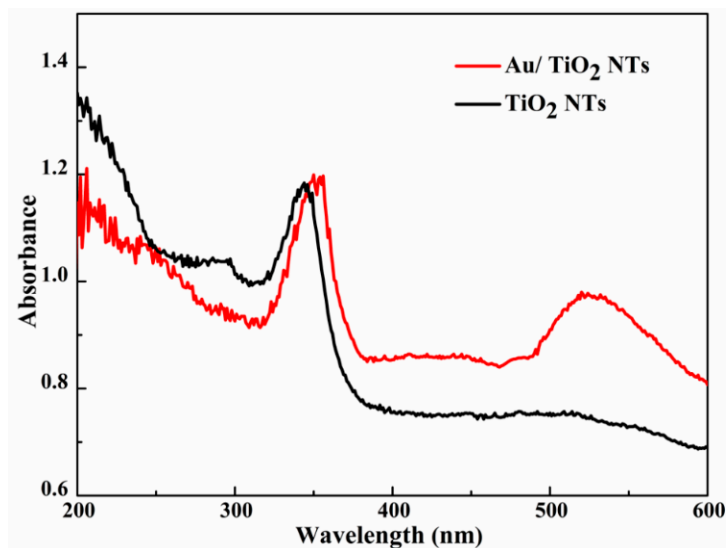

Figure 5. UV-vis DRS spectra of Au/TiO_2 and TiO_2 nanotubes.

The photocatalytic and photoelectrocatalytic performance bestowed by the Au loading on the TiO_2 nanotubes were estimated via the degradation of nitrobenzene solution, a refractory organic wastewater, under room-temperature. The degradation rate curve of nitrobenzene fundamentally corresponded to the first-order kinetic equation ($lnC_0/C_t = k_a t$) in photocatalysis and photoelectrocatalysis, as shown in Figure 6a,b. Significantly, k_a increased gradually with the increase in the Au loading, and k_a decreased as the Au loading

continued to increase. The degradation rates of the nitrobenzene solution with different concentrations are summarized in Figure 6c.
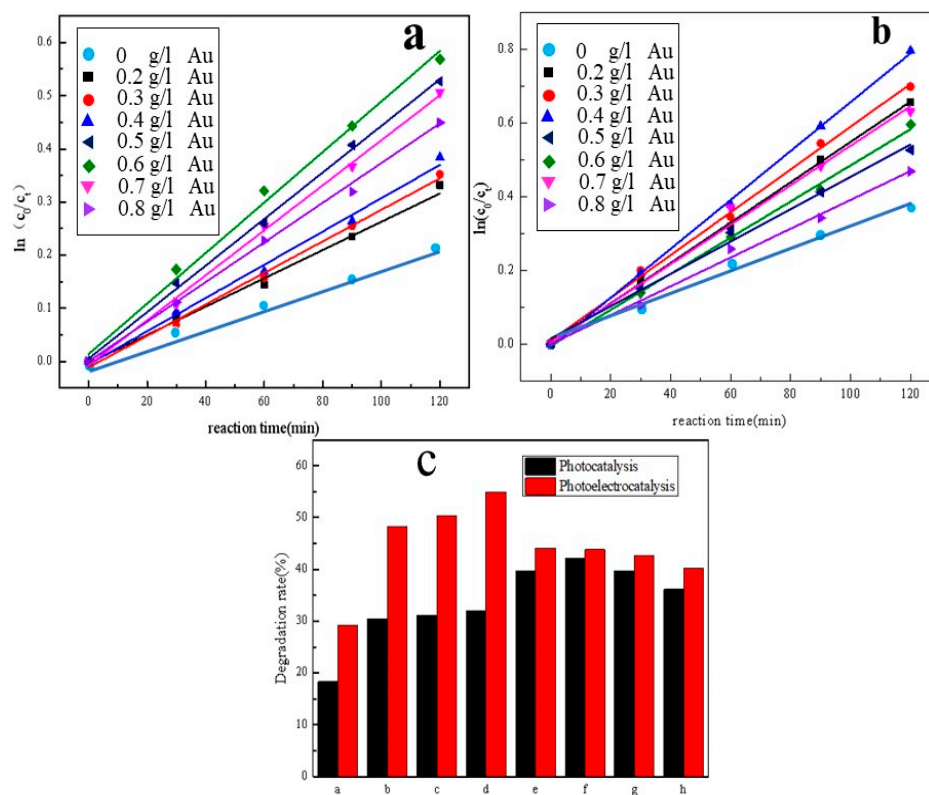

Figure 6. The degradation of nitrobenzene with the prepared samples under the effect of (**a**) photocatalysis and (**b**) photoelectrocatalysis; (**c**) comparison of degradation efficiency between photocatalysis and photoelectrocatalysis.

To determine the optimal Au loading, we prepared samples with varying amounts of Au and induced the photocatalytic degradation of nitrobenzene from wastewater. After a two-hour degradation process, the degradation rates obtained were as follows (shown in Figure 6c (the black bar chart)): 30.50%, 31.09%, 31.92%, 39.71%, 42.24%, 39.70%, and 36.17%. Compared to the 18.35% degradation rate of pristine TiO_2 nanotubes, the efficiency of the Au-loaded TiO_2 nanotubes was higher. However, when the doping concentration reached 0.6 g/L, the degradation effect was optimal among the six different loadings. The results of SEM analysis suggested that excessive Au could obstruct the tube orifices, reducing the transmittance of available light and the number of active sites, ultimately leading to lower degradation efficiency [30].

In Figure 6b, the curve concerns the test of photoelectrocatalytic performance. The data on the degradation of nitrobenzene in Figure 6c (red bar chart) are as follows: 48.21%, 50.35%, 54.90%, 44.07%, 43.79%, 42.70%, and 40.19%. From the above results, it can be gleaned that all the samples of loaded Au were superior to the original TiO_2 nanotubes (29.2%). When the doping concentration reached 0.4 g/L, the degradation efficiency was 54.90%. This can contribute to accelerating the transfer of electrons, restrain the combination of holes with electrons, and extend the life of the hole in the electron–hole pair under applied voltage conditions. However, with a concentration over 0.4 g/L, the efficiency of degradation started to drop. This can be attributed to the mass of Au that will form the Au layer, which is insufficient for the promotion of electrons transfer and the recombination of electron–hole pairs [31]. So, when the loading concentration was 0.4 g/L, the efficiency of photoelectrocatalysis was the best. To improve the efficiency of refractory organic wastewater treatment, photoelectrocatalysis was proposed to enhance the degradation rate. Under the combined action of photocatalysis and bias voltage, the

separation efficiency of the photogenerated charge was improved obviously. At the same time, it can also be seen that the combination of photocatalysis and electrocatalysis allows for better degradation of refractory organic wastewater under lower Au loading conditions.

By analyzing the degradation trend depicted in Figure 7, the rate constant can be determined. As shown in Figure 7a, the degradation rate for the 0.6 g/L Au/TiO$_2$ nanotubes was approximately three times higher than that of the TiO$_2$ nanotubes. Adjusting the Au concentration could enhance the chemical reaction, leading to more effective separation of holes and electrons. In comparison to photocatalysis, the reaction rate was significantly higher with photo-electro coupling. This can be attributed to the presence of more carriers, which, in turn, stimulated more reactions with the target degradation substance.
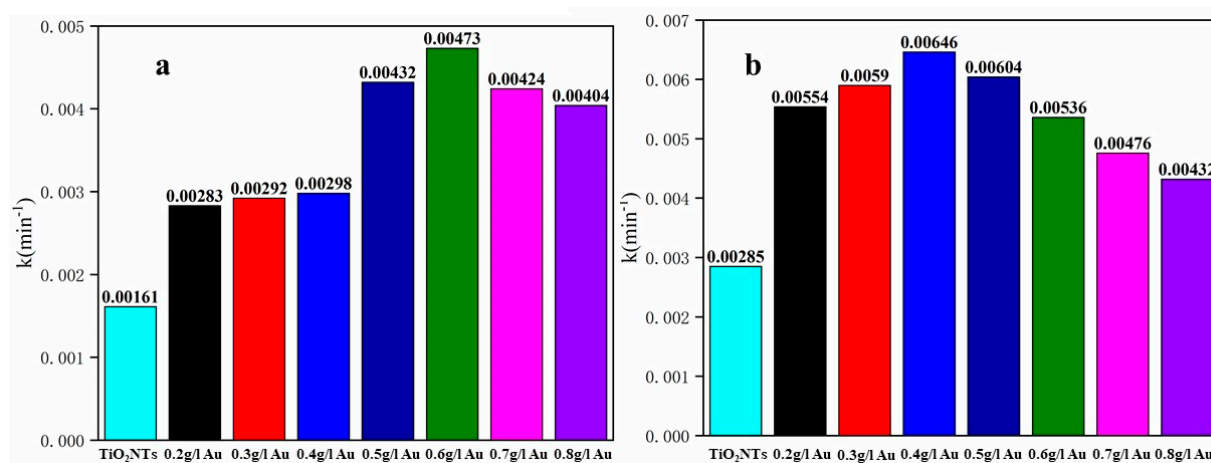

Figure 7. The reaction rate constant of the prepared samples under the effect of (**a**) photocatalysis and (**b**) photoelectrocatalysis.

Maintaining stability in production is crucial for applications. Consequently, the stability of various Au loadings was tested under both PC and PEC conditions, as illustrated in Figure 8. The performance of the modified TiO$_2$ nanotubes was assessed by subjecting the sample to five degradation cycles. The graphs clearly demonstrate that the degradation rate of the sample remained nearly constant, indicating the excellent reusability and stability of the photocatalyst.
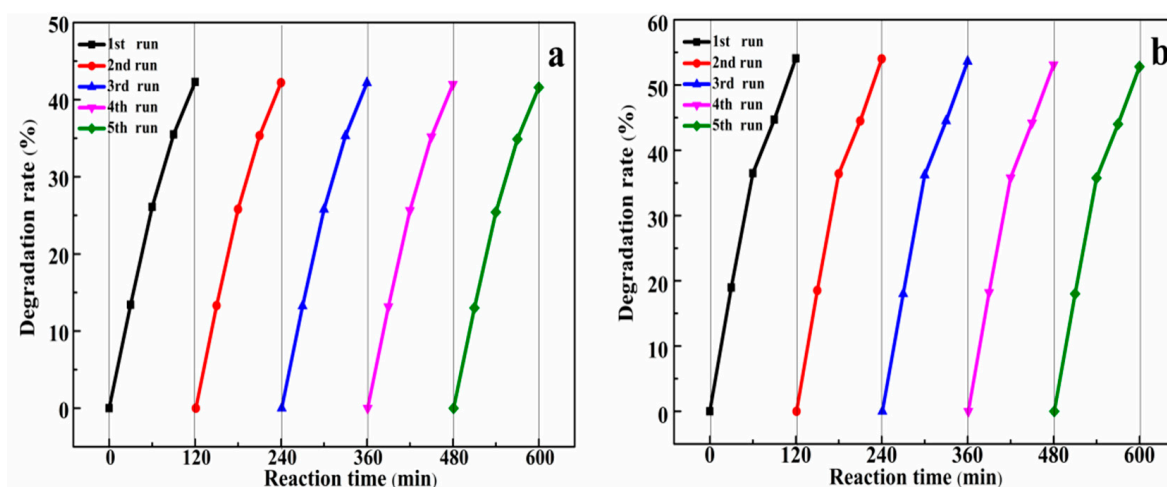

Figure 8. The repeated experiments concerning the use of (**a**) 0.6 g/L Au/TiO$_2$ nanotubes and (**b**) 0.4 g/L Au/TiO$_2$ nanotubes for nitrobenzene degradation.

The potential mechanism behind the enhanced optical performance achieved can be described as follows: Scheme 1a illustrates the photocatalytic degradation mechanism

of nitrobenzene. When Au/TiO$_2$ nanotubes are exposed to ultraviolet light, electrons in the valence band are excited, jumping to the conduction band, while leaving holes in the valence band, ultimately forming electron–hole pairs. Due to the Schottky barrier between the TiO$_2$ nanotubes and Au particles, electrons are induced to move from Au to the conduction band of TiO$_2$, resulting in an increased difference in Fermi energy and ultimately achieving an energy level balance. Furthermore, the oxygen absorbed on the catalyst's surface is restricted by the transferred electrons, leading to the formation of superoxide anions ($\cdot$O^{2-}) [32,33]. Holes in the valence band participate in an oxidation reaction with H$_2$O, forming hydroxyl radicals ($\cdot$OH) [34]. Additionally, due to the SPR effect of the noble metal on the surface, the Au particles become the center of electron capture, further enhancing the separation of the photoinduced electrons and holes and improving the degradation efficiency of nitrobenzene.
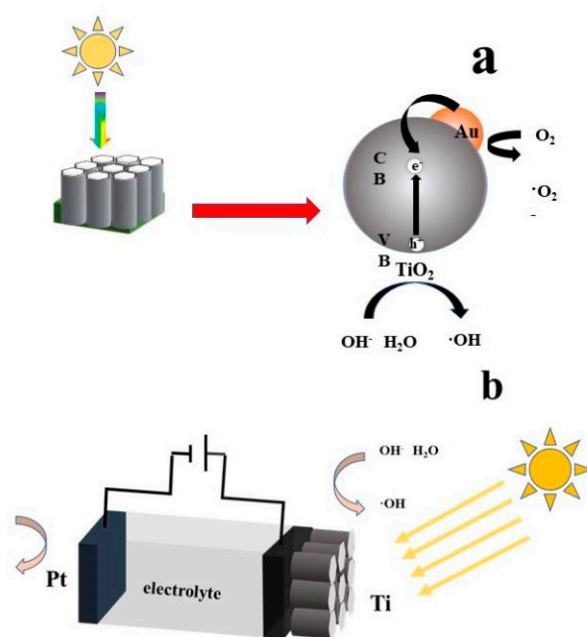
Scheme 1. The mechanism of Au/TiO$_2$ nanotubes under (**a**) photo and (**b**) photo-electro co-induction.

Scheme 1b illustrates the photoelectrocatalytic degradation mechanism of nitrobenzene. Under an applied bias of 1.2 V, the Au/TiO$_2$ nanotubes, serving as a photoanode, undergo an oxidation–reduction reaction. Firstly, the Au/TiO$_2$ nanotubes accelerate the directional movement of photoelectric charge. Secondly, with the application of additional bias voltage, electrons transfer to the Ti substrate along the TiO$_2$ nanotubes, ultimately reaching the counter electrode. This process prolongs the lifetime of the electrons and accelerates the formation of electron–hole pairs, resulting in an increased degradation rate of nitrobenzene. Additionally, since Au/TiO$_2$ nanotubes have a wide absorption band in the visible light region and special optical properties in photocatalysis, it is easier to achieve higher degradation efficiency under natural light conditions, and this is more conducive to their industrial expansion and application in the actual organic wastewater degradation process. Therefore, Au modified TiO$_2$ nanotubes received widespread attention in wastewater degradation.

3. Experimental Procedures

3.1. Chemicals and Instruments

Ti sheet (0.2 mm thick, Strem Chemicals, 99.6%) was cut into a piece that was 20 mm long and 10 mm wide. Ethylene glycol (AR, 99.0%), ammonium fluoride (NH$_4$F, AR), chloroauric acid (HAuCl$_4$·3H$_2$O, AR), acetone (C$_3$H$_6$O, AR), hydrochloric acid (HCl, AR), p-benzoquinone (C$_6$H$_4$O$_2$, AR, 99%), and nitrobenzene (C$_6$H$_5$NO$_2$, AR, 99.0%) were used.

Ultrapure water (resistivity > 18 MΩ·cm) was used in the reaction of nitrobenzene degradation, and the preparation of TiO$_2$ nanotubes and Au/TiO$_2$ nanotubes as shown in Scheme 2; the photocatalyst was put into the quartz beaker with circulating cooling water. Utilizing a 500 W high-pressure mercury lamp as a UV light, the nitrobenzene solution was kept at room temperature and stirred during the photocatalytic reaction process.
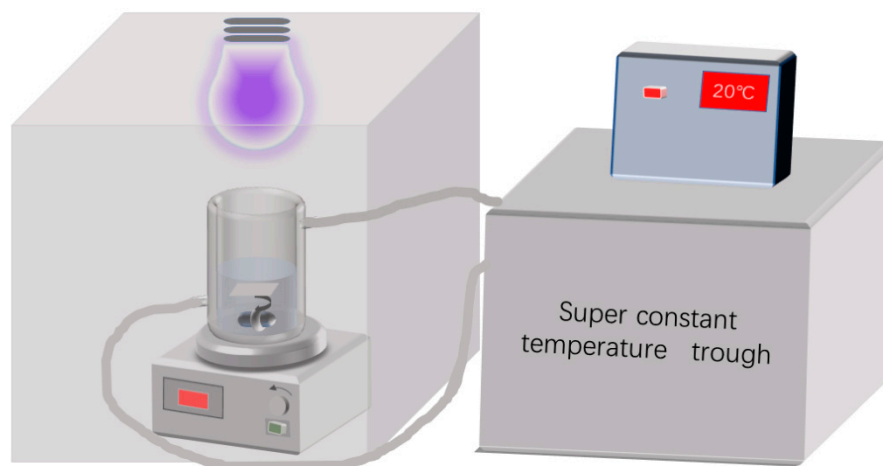
Scheme 2. Reaction equipment used for the degradation of nitrobenzene.

3.2. Preparation of Photocatalyst

TiO$_2$ nanotubes were prepared using a two-step anodization method [35]. The titanium sheets were placed in acetone, ethyl alcohol, hydrochloric acid, and deionized water for sonicating 30 min; and then dried under a pure nitrogen stream. The electrolyte consisted of NH$_4$F (0.5 wt%) in EG with (2 vol%) water. The first-step anodization was conducted for 30 min at 60 V of power. The as-prepared sample was placed in deionized water via sonication treatment, which mainly stripped the thin membrane. Subsequently, the Ti induced the second anodization as above, forming a cellular nanotube structure in the base, and a hexagonal structure on the top layer. Through this two-step anodization, the sample was cleaned and dried with deionized water and then nitrogen stream, respectively. Then, the prepared sample was calcined for 1h in a muffle furnace, maintained at a temperature of 450 °C, with heating rate at 5 °C/min, and cooled at room temperature. Using chloroauric acid as the gold source, different concentrations of electrolyte were prepared, including 0.2–0.8 g/L of HAuCl$_4$·4H$_2$O. Au/TiO$_2$ nanotubes were prepared as follows: TiO$_2$ was used as the cathode, and Pt sheet was used as the anode. The Au/TiO$_2$ nanotubes were prepared using an electrochemical reduction method at a fixed electrode potential of 1.2 V in solutions with different concentrations for 10 min. Then, the Au/TiO$_2$ nanotubes were removed and dried at room temperature.

3.3. Experiment Ways

In the photocatalytic degradation experiment, a high-pressure mercury lamp with a radiation distance of 10 cm was used as the light source to simulate the ultraviolet part of the sunlight and irritate the organic wastewater (30 mL, 200 mg/L of nitrobenzene; 0.5 g/L of Na$_2$SO$_4$). For photoelectrocatalysis, the bias voltage was kept constant at 1.2 V, with Au/TiO$_2$ nanotubes serving as the photoanode and Pt serving as the photocathode. Each experiment was repeated 3 times, and the average and standard errors were calculated.

3.4. Characterization of Catalyst

The surface morphology and distribution of the nanotubes loaded with Au nanoparticles were analyzed utilizing a scanning electron microscope (SEM, Zeiss, Oberkochen, Germany, Sigma HV). The relevant chemical components of TiO$_2$ nanotubes and Au-loaded nanotubes were detected using an energy dispersive spectrometer (EDS). The crystal form

of catalysis was examined via X-ray diffraction (XRD, Rigaku, Tokyo, Japan, D/MAX2200) with Cu Ka resource. The bulk elemental composition was determined using Inductively coupled plasma atomic emission spectrometer (ICP-AES, Agilent 730, Agilent, Santa Clara, CA, USA). For analysis, the samples were dissolved in aquaregia and subsequently diluted to a fixed volume of 50 mL prior to detection.

Utilizing the degradation of nitrobenzene, we were able to estimate the photocatalytic activity and stability of the sample at room temperature. The absorbance of nitrobenzene was measured using a UV spectrophotometer after degradation each 30 min for 2 h. The concentration of nitrobenzene with the corresponding time was calculated using the standard graph. Nitrobenzene has a characteristic absorption peak in the ultraviolet region. The absorbance of nitrobenzene solutions at 25, 50, 100, 150, and 200 mg/L was measured using a stepwise dilution method. The measurement results are shown in Figure 9a. As shown in the figure, the nitrobenzene solution exhibited a relatively obvious absorption peak at around 265 nm. Using the measured absorbance as the vertical axis and the corresponding nitrobenzene concentration as the horizontal axis, the relationship between nitrobenzene concentration and absorbance was obtained. The standard curve was plotted, as shown in Figure 9b:
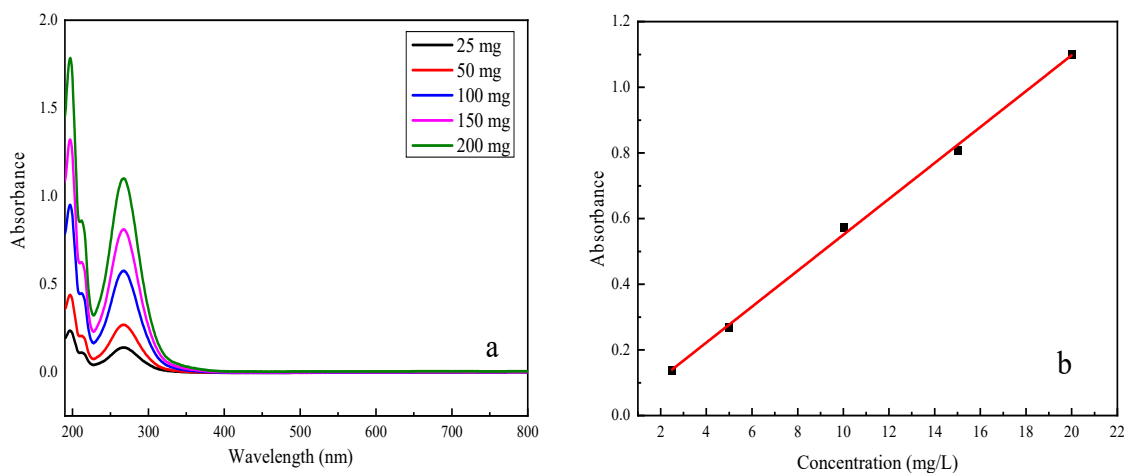

Figure 9. UV absorption curve (**a**) and absorbance–concentration standard curve (**b**) of nitrobenzene standard solution.

4. Conclusions

In summary, a catalyst was synthesized using the electrochemical deposition method, resulting in the formation of Au/TiO_2 nanotubes with varying doping concentrations. These nanotubes exhibited favorable photocatalytic (PC) and enhanced photoelectrocatalytic (PEC) properties, surpassing those of pure TiO_2, toward the degradation of nitrobenzene. The successful deposition of Au onto the TiO_2 surface was confirmed by the collected data. The catalytic activity was assessed by measuring the degradation of nitrobenzene, and the optimal PC and PEC performances were observed at concentrations of 0.6 g/L and 0.4 g/L, respectively. The improved PC/PEC performance can be attributed to the presence of Au nanoparticles, which expanded the response range to visible light, enhanced the efficiency of photoelectric hole separation, and suppressed charge recombination. Notably, the degradation efficiency surpassed that of photocatalysis at the same doping concentration under a photoelectric field. Based on its superior photoelectro performance, this catalyst holds promising potential for practical applications in environmental protection.

Author Contributions: Conceptualization, D.G. and B.W.; methodology, D.G.; validation, M.W., C.L. and Y.W.; investigation, M.W.; data curation, C.L.; writing—original draft preparation, M.W. and C.L.; writing—review and editing, M.W.; supervision, B.W.; funding acquisition, D.G. All authors have read and agreed to the published version of the manuscript.

Data Availability Statement: The data that support this study are available in the article.

Conflicts of Interest: The authors declare that they have no known competing financial interests or personal relationships that could have appeared to influence the work reported in this paper.

References

1. Di, G.; Shixu, Z.; Tingting, J.; Hong, J.; Xirui, W.; Baohui, W. Positive P/g-C_3N_4 thermo-coupled photocatalytic oxidation of refractory organics in wastewater for total utilization of solar Vis-IR region. *Mater. Chem. Phys.* **2020**, *253*, 123307. [CrossRef]

2. Jo, W.-K.; Natarajan, T.S. Influence of TiO_2 morphology on the photocatalytic efficiency of direct Z-scheme g-C_3N_4/TiO_2 photocatalysts for isoniazid degradation. *Chem. Eng. J.* **2015**, *281*, 549–565. [CrossRef]

3. Eid, K.; Sliem, M.H.; Abdullah, A.M. Tailoring the defects of sub-100 nm multipodal titanium nitride/oxynitride nanotubes for efficient water splitting performance. *Nanoscale Adv.* **2021**, *3*, 5016–5026. [CrossRef] [PubMed]

4. Xie, K.; Sun, L.; Wang, C.; Lai, Y.; Wang, M.; Chen, H.; Lin, C. Photoelectrocatalytic properties of Ag nanoparticles loaded TiO_2 nanotube arrays prepared by pulse current deposition. *Electrochim. Acta* **2010**, *55*, 7211–7218. [CrossRef]

5. Chong, X.; Zhao, B.; Li, R.; Ruan, W.; Yang, X. Photocatalytic degradation of rhodamine 6G on Ag modified TiO_2 nanotubes: Surface-enhanced Raman scattering study on catalytic kinetics and substrate recyclability. *Colloids Surf. A Physicochem. Eng. Asp.* **2015**, *481*, 7–12. [CrossRef]

6. Xing, L.; Jia, J.; Wang, Y.; Zhang, B.; Dong, S. Pt modified TiO_2 nanotubes electrode: Preparation and electrocatalytic application for methanol oxidation. *Int. J. Hydrogen Energy* **2010**, *35*, 12169–12173. [CrossRef]

7. Shang-Hau, C.; Hsin-Chia, H.; Han-Ting, L.; Feng-Yu, T.; Chun-Wen, T.; Yung-Jung, H.; Chun-Hway, H. Plasmonic gold nanoplates-decorated ZnO branched nanorods@TiO_2 nanorods heterostructure photoanode for efficient photoelectrochemical water splitting. *J. Photochem. Photobiol. A Chem.* **2023**, *443*, 114816. [CrossRef]

8. Tran, T.T.H.; Tran, T.K.C.; Le, T.Q.X. Engineering the surface structure of brookite-TiO_2 nanocrystals with Au nanoparticles by cold-plasma technique and its photocatalytic and self-cleaning property. *J. Nanopart Res.* **2023**, *25*, 203. [CrossRef]

9. Crişan, D.; Drăgan, N.; Răileanu, M.; Crişan, M.; Ianculescu, A.; Luca, D.; Năstuţă, A.; Mardare, D. Structural study of sol–gel Au/TiO_2 films from nanopowders. *Appl. Surf. Sci.* **2011**, *257*, 4227–4231. [CrossRef]

10. Li, Y.; Yu, H.; Zhang, C.; Fu, L.; Li, G.; Shao, Z.; Yi, B. Enhancement of photoelectrochemical response by Au modified in TiO_2 nanorods. *Int. J. Hydrogen Energy* **2013**, *38*, 13023–13030. [CrossRef]

11. Wang, C.; Wang, F.; Xu, M.; Zhu, C.; Fang, W.; Wei, Y. Electrocatalytic degradation of methylene blue on Co doped Ti/TiO_2 nanotube/PbO_2 anodes prepared by pulse electrodeposition. *J. Electroanal. Chem.* **2015**, *759*, 158–166. [CrossRef]

12. Chen, X.; Jiang, H.; Cui, D.; Lu, K.; Kong, X.; Cai, J.; Yu, S.; Zhang, X. Selectivity Regulation of Au/Titanate by Biochar Modification for Selective Oxidation of Benzyl Alcohol. *Catalysts* **2023**, *13*, 864. [CrossRef]

13. Zhao, Y.; Hoivik, N.; Akram, M.N.; Wang, K. Study of plasmonics induced optical absorption enhancement of Au embedded in titanium dioxide nanohole arrays. *Opt. Mater. Express* **2017**, *7*, 2871–2879. [CrossRef]

14. Molinari, R.; Lavorato, C.; Argurio, P. Photocatalytic reduction of acetophenone in membrane reactors under UV and visible light using TiO_2 and Pd/TiO_2 catalysts. *Chem. Eng. J.* **2015**, *274*, 307–316. [CrossRef]

15. Liao, W.; Yang, J.; Zhou, H.; Murugananthan, M.; Zhang, Y. Electrochemically Self-Doped TiO_2 Nanotube Arrays for Efficient Visible Light Photoelectrocatalytic Degradation of Contaminants. *Electrochim. Acta* **2014**, *136*, 310–317. [CrossRef]

16. Xiao, F.X.; Miao, J.; Tao, H.B.; Hung, S.F.; Wang, H.Y.; Yang, H.B.; Chen, J.; Chen, R.; Liu, B. One-dimensional hybrid nanostructures for heterogeneous photocatalysis and photoelectrocatalysis. *Small* **2015**, *11*, 2115–2131. [CrossRef]

17. Thabit, M.; Liu, H.; Zhang, J.; Wang, B. Pd-MnO_2 nanoparticles/TiO_2 nanotube arrays (NTAs) photo-electrodes photo-catalytic properties and their ability of degrading Rhodamine B under visible light. *J. Environ. Sci.* **2017**, *60*, 53–60. [CrossRef]

18. Yang, L.; Zheng, X.; Liu, M.; Luo, S.; Luo, Y.; Li, G. Fast photoelectro-reduction of Cr(VI) over MoS_2@TiO_2 nanotubes on Ti wire. *J. Hazard. Mater.* **2017**, *329*, 230–240. [CrossRef]

19. Gao, B.; Zhao, X.; Liang, Z.; Wu, Z.; Wang, W.; Han, D.; Niu, L. CdS/TiO_2 Nanocomposite-Based Photoelectrochemical Sensor for a Sensitive Determination of Nitrite in Principle of Etching Reaction. *Anal. Chem.* **2021**, *93*, 820–827. [CrossRef]

20. Gong, J.; Pu, W.; Yang, C.; Zhang, J. A simple electrochemical oxidation method to prepare highly ordered Cr-doped titania nanotube arrays with promoted photoelectrochemical property. *Electrochim. Acta* **2012**, *68*, 178–183. [CrossRef]

21. Jing, L.; Tan, H.L.; Amal, R.; Ng, Y.H.; Sun, K.-N. Polyurethane sponge facilitating highly dispersed TiO_2 nanoparticles on reduced graphene oxide sheets for enhanced photoelectro-oxidation of ethanol. *J. Mater. Chem. A* **2015**, *3*, 15675–15682. [CrossRef]

22. Kejia, W.; Minglong, C.; Qiang, Z.; Xuehui, L. Radical and (photo)electron transfer induced mechanisms for lignin photo-and electro-catalytic depolymerization. *Green Energy Environ.* **2023**, *8*, 383–405. [CrossRef]

23. Mohamed, M.M. Gold loaded titanium dioxide–carbon nanotube composites as active photocatalysts for cyclohexane oxidation at ambient conditions. *RSC Adv.* **2015**, *5*, 46405–46414. [CrossRef]

24. Wang, H.; Qin, P.; Yi, G.; Zu, X.; Zhang, L.; Hong, W.; Chen, X. A high-sensitive ultraviolet photodetector composed of double-layered TiO_2 nanostructure and Au nanoparticles film based on Schottky junction. *Mater. Chem. Phys.* **2017**, *194*, 42–48. [CrossRef]

25. Ghorbani, V.; Dorranian, D. Properties of TiO_2/Au nanocomposite produced by pulsed laser irradiation of mixture of individual colloids. *Appl. Phys. A* **2016**, *122*, 1019. [CrossRef]

26. Moazeni, M.; Hajipour, H.; Askari, M.; Nusheh, M. Hydrothermal synthesis and characterization of titanium dioxide nanotubes as novel lithium adsorbents. *Mater. Res. Bull.* **2015**, *61*, 70–75. [CrossRef]

27. Yun, J.-W.; Nguyen, T.K.; Lee, S.; Kim, S.; Kim, Y.S.; Nguyen, T.K.; Nguyen, C.K.; Ha, Y. Enhanced Plasmonic Electron Transfer from Gold Nanoparticles to TiO_2 Nanorods via Electrochemical Surface Reduction. *J. Korean Phys. Soc.* **2020**, *77*, 853–860. [CrossRef]

28. Eri, F.; Yusuke, K.; Ryuto, O.; Atsuhiro, T.; Hiroshi, K. One-pot synthesis of secondary amines from aldehydes and primary amines over trifunctional Au-TiO_2 as a water adsorbent, acid catalyst and photocatalyst without the use of hydrogen gas. *Appl. Catal. A Gen.* **2023**, *657*, 119156. [CrossRef]

29. Van Viet, P.; Trung, N.C.; Nhut, P.M.; Van Hieu, L.; Thi, C.M. The fabrication of the antibacterial paste based on TiO_2 nanotubes and Ag nanoparticles-loaded TiO_2 nanotubes powders. *J. Exp. Nanosci.* **2017**, *12*, 220–231. [CrossRef]

30. Fu, F.; Zhang, Y.; Zhang, Z.; Zhang, X.; Chen, Y.; Zhang, Y. The preparation and performance of Au loads TiO_2 nanomaterials. *Mater. Res. Express* **2019**, *6*, 095041. [CrossRef]

31. Jansanthea, P.; Chomkitichai, W.; Ketwaraporn, J.; Pookmanee, P.; Phanichphant, S. Flame spray pyrolysis synthesized gold-loaded titanium dioxide photocatalyst for degradation of Rhodamine B. *J. Aust. Ceram. Soc.* **2018**, *55*, 719–727. [CrossRef]

32. Xu, Z.; Lin, Y.; Yin, M.; Zhang, H.; Cheng, C.; Lu, L.; Xue, X.; Fan, H.J.; Chen, X.; Li, D. Understanding the Enhancement Mechanisms of Surface Plasmon-Mediated Photoelectrochemical Electrodes: A Case Study on Au Nanoparticle Decorated TiO_2 Nanotubes. *Adv. Mater. Interfaces* **2015**, *2*, 1500169. [CrossRef]

33. Venkata Seshaiah, K.; Vishnuvardhan Reddy, C.; Sai Santosh Kumar, R. Plasmonic Au NPs embedded Ytterbium-doped TiO_2 nanocomposites photoanodes for efficient indoor photovoltaic devices. *Appl. Surf. Sci.* **2023**, *611*, 155728. [CrossRef]

34. João, L.; Eva, D.; Pawel, M.; Magdalena, M.; Tomasz, K.; Adriana, Z.; Rui, C.M.; João, G. The role of noble metals in TiO_2 nanotubes for the abatement of parabens by photocatalysis, catalytic and photocatalytic ozonation. *Sep. Purif. Technol.* **2023**, *326*, 124747. [CrossRef]

35. Di, G.; Shixu, Z.; Tingting, J.; Hong, J.; Baohui, W.; Xirui, W. E-carbon antenna-assembled TiO_2 nanotubes for sensitization of photocatalytic reaction exemplified by enhanced oxidation of nitrobenzene. *Chem. Eng. J.* **2019**, *375*, 121992. [CrossRef]